View metadata, citation and similar papers at core.ac.uk
brought to you by CORE
provided by RERO DOC Digital Library

J Biomol NMR (2013) 56:149–154
DOI 10.1007/s10858-013-9731-0

ARTICLE

4D experiments measured with APSY for automated backbone resonance assignments of large proteins

Barbara Krähenbühl · Julien Boudet · Gerhard Wider

Received: 17 January 2013 / Accepted: 16 April 2013 / Published online: 30 April 2013
© Springer Science+Business Media Dordrecht 2013

Abstract Detailed structural and functional characterization of proteins by solution NMR requires sequence-specific resonance assignment. We present a set of transverse relaxation optimization (TROSY) based four-dimensional automated projection spectroscopy (APSY) experiments which are designed for resonance assignments of proteins with a size up to 40 kDa, namely HNCACO, HNCOCA, HNCACB and HN(CO)CACB. These higher-dimensional experiments include several sensitivity-optimizing features such as multiple quantum parallel evolution in a 'just-in-time' manner, aliased off-resonance evolution, evolution-time optimized APSY acquisition, selective water-handling and TROSY. The experiments were acquired within the concept of APSY, but they can also be used within the framework of sparsely sampled experiments. The multidimensional peak lists derived with APSY provided chemical shifts with an approximately 20 times higher precision than conventional methods usually do, and allowed the assignment of 90 % of the backbone resonances of the perdeuterated primase-polymerase ORF904, which contains 331 amino acid residues and has a molecular weight of 38.4 kDa.

Keywords Automated projection spectroscopy · APSY · GAPRO · TROSY · JIT · MQ parallel evolution

Electronic supplementary material The online version of this article (doi:10.1007/s10858-013-9731-0) contains supplementary material, which is available to authorized users.

B. Krähenbühl · J. Boudet · G. Wider (✉)
Institute of Molecular Biology and Biophysics, ETH Zurich, 8093 Zurich, Switzerland
e-mail: gsw@mol.biol.ethz.ch

Introduction

A detailed analysis of NMR spectra requires the assignment of the resonances to the corresponding nuclei; a procedure which can be quite tedious. In particular spectra of large proteins suffer from signal overlap in the commonly acquired 2D and 3D experiments, which makes resonance assignment with these spectra time-consuming and labor-intensive. The advent of novel sampling methods has opened new perspectives with respect to dimensionality and resolution of NMR experiments (Kim and Szyperski 2003; Szyperski et al. 1993; Kupce and Freeman 2003; Orekhov et al. 2003; Coggins and Zhou 2006; Kazimierczuk et al. 2006; Jaravine et al. 2008). Automated projection spectroscopy (APSY) (Hiller et al. 2005a, 2008b; Hiller and Wider 2011; Krähenbühl and Wider 2012) provides an efficient method for the measurement and analysis of higher-dimensional experiments. The algorithm GAPRO, the key element of APSY, calculates the original frequencies of the resonances in the higher-dimensional frequency space from the peaks picked in 2D projection spectra. APSY has proven to provide with this procedure accurate, artifact-free and precise peak lists due to statistical selection and averaging effects. These high quality peak lists are an ideal basis for automated resonance assignments (Fiorito et al. 2006; Hiller et al. 2007, 2008a; Gossert et al. 2011; Krähenbühl et al. 2011; Narayanan et al. 2010).

Automated assignment procedures based on APSY were so far limited to globular proteins with molecular weights below 20 kDa, or when deuterated just above 20 kDa for backbone resonance assignments (Gossert et al. 2011). Using transverse relaxation optimized spectroscopy (TROSY) (Pervushin et al. 1997) and further optimized experimental schemes we could significantly increase the

molecular weight of proteins for which backbone and $^{13}C^{\beta}$ resonance assignments can be obtained with APSY. In the following we present two sets of two mutually complementing experiments. In principle, both pairs of experiments supply the necessary data; but depending on the particular application either of them provides specific advantages. One set consists of 4D TROSY APSY-HNCACB and -HN(CO)CACB experiments. These experiments result directly in two 4D peak lists which can be correlated to identify the self and sequential $^{13}C^{\alpha}_{i/i-1}$, $^{13}C'_{i/i-1}$ chemical shifts for a pair of $^{1}H^{N}_{i}$ and $^{15}N_{i}$ nuclei, and subsequently be connected for sequential resonance assignment by correlating the $^{13}C^{\alpha}$ and $^{13}C^{\beta}$ chemical shifts. Further, 4D TROSY APSY-HNCOCA and -HNCACO experiments are presented, which can be used similarly, by correlating via the $^{1}H^{N}$–^{15}N and $^{13}C^{\alpha}$–$^{13}C'$ chemical shifts (Fig. 1). In the conventional 3D implementation the latter set can hardly be used for sequential assignments of resonances: The matching occurs via the $^{1}H^{N}$–^{15}N on one side, but only via $^{13}C^{\alpha}$ on the other. This situation is released in the APSY implementation where two pairs of two very precise frequencies are available for matching. The different sets of experiments have intrinsic features which differentiate their potential applications (see "Results and Discussion").

Materials and methods

Sample preparation

The TROSY APSY experiments were performed on the uniformly [^{2}H, ^{13}C, ^{15}N]–labeled archeo-eukaryotic primase-polymerase of the plasmid pRN1, ORF904 (Beck et al. 2010), which contains 331 amino acids (including 14 prolines) and has a calculated molecular weight of 38.4 kDa. The secondary structure of the protein consists of 15 % β-sheets and 42 % α-helices. ORF904 was obtained from overexpression in *E. coli* grown in M9 minimal medium (99 % D_2O) containing [^{2}H, ^{13}C] glucose and $^{15}NH_4Cl$ as deuterium/carbon and nitrogen sources, respectively (Gardner and Kay 1998). For the data collection, the final concentration of the protein in H_2O:D_2O 95:5 (v:v) was 0.75 mM as measured by PULCON (Wider and Dreier 2006). The buffer was 25 mM sodium acetate, 75 mM NaCl, 2 mM β-mercaptoethanol, 1 mM EDTA and NaN_3 at pH 5.4. ROCHE® protease inhibitor cocktail was added. ORF904 is highly stable and its compact fold required approximately 4 weeks at 323 K for the back-exchange of all amide protons.

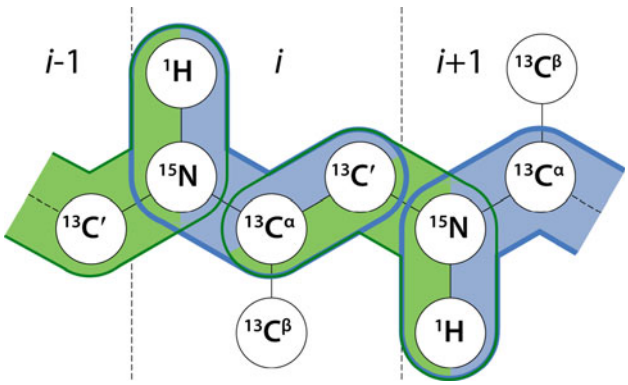

Fig. 1 Schematic representation of the automated assignment procedure with the peak lists of a 4D TROSY APSY-HNCACO (*blue*) and a 4D TROSY APSY-HNCOCA experiment (*green*). For sequence-specific assignment the peak lists are matched via $^{1}H^{N}$–^{15}N and $^{13}C^{\alpha}$–$^{13}C'$ chemical shift pairs. *i*, *i*−1 and *i*+1 indicate consecutive residues

Description of the pulse sequences

The pulse sequences of the experiments were optimized for large proteins by including features which improve both sensitivity and resolution. The 4D TROSY APSY-HNCACO pulse sequence (Fig. 2) is based on a 3D JIT HN(CA)CO experiment (Werner-Allen et al. 2006) which includes [^{15}N–$^{1}H^{N}$]-TROSY and a multiple quantum (MQ) evolution of $^{13}C'$ coherence with respect to $^{13}C^{\alpha}$. A discussion of the high sensitivity of this approach has been presented before (Werner-Allen et al. 2006) and included detailed comparisons with conventional TROSY experiments. For our purpose we extended the constant-time ^{15}N evolution period into a semi constant-time period that allows higher resolution when required.

In addition to the sensitivity advantage, the JIT-based pulse sequence proved ideal for the inclusion of a $^{13}C^{\alpha}$ evolution for a 4D experiment (Fig. 2): The full period with transversal $^{13}C^{\alpha}$, which includes the two $^{13}C^{\alpha}$–$^{13}C'$ transfer periods and the $^{13}C^{\alpha}$/$^{13}C'$ MQ element with $^{13}C'$ evolution, can be used for $^{13}C^{\alpha}$ evolution. Maximal evolution times of 16.4 and 25 ms can be obtained for projections with only $^{13}C^{\alpha}$ and simultaneous $^{13}C^{\alpha}$ and $^{13}C'$ evolution, respectively. If conventional 3D TROSY HN(CA)CO sequences without the JIT elements would have been modified to a 4D sequence with $^{13}C^{\alpha}$ evolution, as has been published before (Konrat et al. 1999; Yang and Kay 1999), the evolution time would be limited to one $^{13}C^{\alpha}$–$^{13}C'$ transfer period (8.6 ms), and would be modulated by J-coupling to $^{13}C^{\beta}$ (Werner-Allen et al. 2006). The sensitivity could be further improved with respect to the underlying 3D 'just-in-time' sequence by replacing the TROSY element with the ST2-PT (single transition-to-single transition polarization transfer) TROSY variant (Pervushin et al. 1998; Salzmann et al. 1999), the partial replacement of the sinc-shaped pulses on $^{13}C'$ with

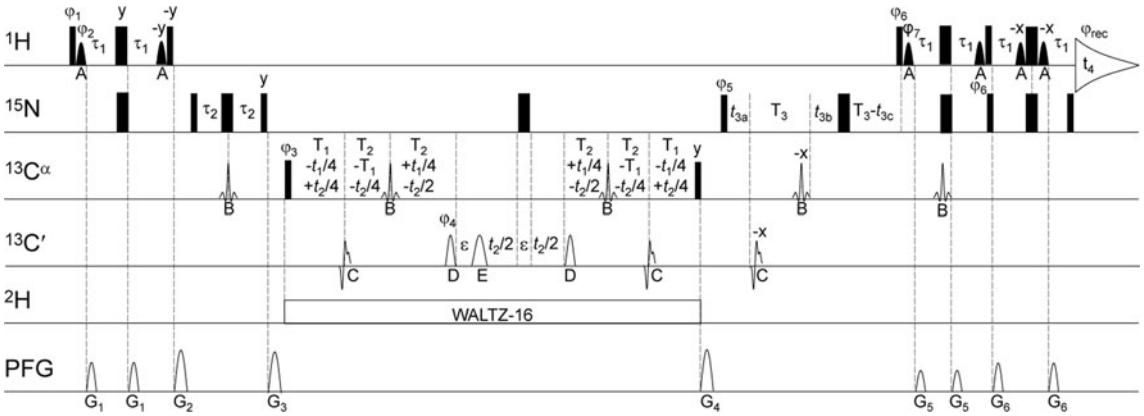

Fig. 2 Pulse sequence of the 4D TROSY APSY-HNCACO experiment (APSY one-letter code: aoNH). *Black thin* and *wide rectangular bars* represent 90° and 180° high-power pulses, respectively. The carrier frequencies were set to 4.7, 118, 56, and 3.8 ppm on the ^{1}H, ^{15}N, ^{13}C, and ^{2}H channel, respectively. $^{13}C^{\alpha}$ is decoupled from ^{2}H with WALTZ-16 (Shaka et al. 1983). The time periods were $\tau_1 = 2.4$ ms, $\tau_2 = 12.5$ ms, $T_1 = 4.3$ ms, $T_2 = 7.1$ ms—$\Delta/2$ with Δ = pulse durations D + C + 180° ^{15}N, $\varepsilon = 180°$ ^{15}N, $T_3 = \tau_2 - \tau_1 = 10.1$ ms, and initial values of 0 µs for all evolution periods. The pulses labeled with *a* are selective 180° Sinc (*central lobe*) pulses on water protons with a length of 1 ms; *b* are off-resonance 180° Reburp (Geen and Freeman 1991) pulses with a duration of 375 µs applied on $^{13}C^{ali}$ at 44 ppm; *c* are 180° Gaussian cascades (Q3) (Emsley and Bodenhausen 1990) with a duration of 309 µs, off-resonance on $^{13}C'$ at 177 ppm; pulses *d* and *e* are selective off-resonance $^{13}C'$ pulses, with *d* being a 90° Sinc pulse with duration 378 µs, and *e* being a 180° Sinc (*central lobe*) pulse with duration 309 µs on a 700 MHz spectrometer. All pulses were applied along the *x-axis* unless indicated otherwise above the pulse symbol. The following phase cycles were used: $\varphi_1 = 2(x), 2(-x)$; $\varphi_2 = -\varphi_1$; $\varphi_3 = 4(x), 8(-x), 4(x)$; $\varphi_4 = 4(x), 4(-x)$; $\varphi_5 = -x, -y$ or $-x, y$ (for *even or odd number* of increments); $\varphi_6 = -y$; $\varphi_7 = -\varphi_6$; $\varphi_{rec} = \alpha, 2(-\alpha), \alpha$ (receiver phase) with $\alpha = -y, x, y, -x$. Quadrature detection for the indirect dimensions was achieved for $t_1(^{13}C^{\alpha})$ and $t_2(^{13}C')$ by States-TPPI (Marion et al. 1989) incrementing phases φ_3 and φ_4, and for $t_3(^{15}N)$ by the echo-antiecho method (Kay et al. 1992) incrementing φ_5, φ_6 and φ_7. For $^{13}C^{\alpha}$ constant time, and for ^{15}N semi-constant time evolution periods were used. The trigonometric addition theorem was used to obtain pure cosine and sine terms for a subsequent hypercomplex Fourier transformation (Brutscher et al. 1995; Kupce and Freeman 2003). The sine-bell shaped pulsed field gradient (PFG) pulses were applied with a length of 800 µs and the following strengths: G_1: 10.5 G/cm; G_2: 27.5 G/cm; G_3: 33 G/cm; G_4: 40.2 G/cm; G_5: 8.3 G/cm; G_6: 17.6 G/cm

Gaussian cascades (Emsley and Bodenhausen 1990), and a refined water-handling procedure which keeps the solvent magnetization longitudinal whenever possible (Hiller et al. 2005b; Grzesiek and Bax 1993).

As a result of the simultaneous MQ evolution of $^{13}C^{\alpha}$ and $^{13}C'$, the $^{13}C'$ resonances are measured while the carrier frequency is set to the $^{13}C^{\alpha}$ offset, Ω_{CA} (approx. 56 ppm). The $^{13}C'$ signals are thus aliased into the $^{13}C^{\alpha}$ spectral region. To preserve the $^{13}C'$ signal pattern, the sweep width in the $^{13}C'$ dimension must be an integer fraction of the difference Ω_{CO}–Ω_{CA}, where Ω_{CO} is the carbonyl offset. In general, when in the indirect dimension resonances of other nuclei evolve simultaneously to $^{13}C'$ resonances, the condition

$$in_{tot}\sin(\alpha)(\Omega_{CO} - \Omega_{CA}) \in \mathbb{N}$$

must be fulfilled, where in_{tot} is the inverse of the sweep width in this projection, α is the projection angle for $^{13}C'$, i.e., $in_{tot}\sin(\alpha)$ is the specific increment of $^{13}C'$.

The pulse sequence of the 4D TROSY APSY-HNCOCA experiment is very similar to the 4D TROSY APSY-HNCACO pulse sequence, including ST2-PT and MQ parallel evolution, except that the roles of $^{13}C^{\alpha}$ and $^{13}C'$ are interchanged, and no constant-time period is used to decouple $^{13}C^{\alpha}$ from $^{13}C^{\beta}$. The advantage with respect to a conventional 4D version with SQ evolution is not as significant as for the 4D TROSY APSY-HNCACO experiment; however, the possibility of a long constant-time $^{13}C'$ evolution, utilizing the transfer periods, makes the MQ parallel evolution attractive for fields up to 700 MHz, where CSA does not dominate the relaxation of $^{13}C'$.

For both 4D TROSY APSY-HNCACB and -HN(CO)-CACB experiments, the $^{1}H^{N}/^{15}N$ pulse sequence elements are identical to the ones used in the other set of experiments (see Supplementary Material), and the $^{13}C^{\alpha}/^{13}C^{\beta}$ elements are very similar to the corresponding parts in the published 4D APSY-HNCACB (Gossert et al. 2011).

Data acquisition and processing

All experiments were measured at 323 K on a Bruker 700 MHz Avance III spectrometer with cryogenic probe, z-gradient accessory and operating software Topspin 2.1 (Bruker, Karlsruhe, Germany). For the 4D TROSY APSY-HNCACO, 33 projections were measured within 33 h, and for the 4D TROSY APSY-HNCOCA 33 projections within 20 h. The 4D TROSY APSY-HNCACB experiment was measured with 35 projections within 30 h, and the 4D TROSY APSY-HN(CO)CACB experiment was measured

with 29 projections within 33 h. After automated serial processing of the 2D projections with Prosa 6.1 (Güntert et al. 1992), peaks were picked in the projection spectra by GAPRO (Hiller et al. 2005a) which further calculated from these 2D peak lists the 4D peak positions. The 4D TROSY APSY-HNCACO and 4D TROSY APSY-HNCOCA peak lists were merged with MATLAB (R2010b, The MathWorks, Natick, MA, USA) based on the chemical shifts of the $^{1}H^{N}$–^{15}N moieties to an inter-residue 6D $^{13}C^{\alpha}_{i-1}$–$^{13}C'_{i-1}$–$^{1}H^{N}_{i}$–$^{15}N_{i}$–$^{13}C^{\alpha}_{i}$–$^{13}C'_{i}$ peak list. As correlation criteria, threshold ellipses were used. The elliptical approach makes the matching conditions for the different dimensions interdependent, i.e., values close to the threshold in one dimension are passing only when the other dimensions are more precise. The 4D TROSY APSY-HNCACB and -HN(CO)CACB peak lists were merged correspondingly to a 6D $^{13}C^{\alpha}_{i-1}$–$^{13}C^{\beta}_{i-1}$–$^{1}H^{N}_{i}$–$^{15}N_{i}$–$^{13}C^{\alpha}_{i}$–$^{13}C^{\beta}_{i}$ peak list. These 6D chemical shift lists were used as input for MARS (Jung and Zweckstetter 2004) or UNIO/MATCH (Volk et al. 2008) for subsequent sequential resonance assignment strategies. Detailed parameters of the measurement and analysis of the experiments are provided in the Supplementary Material.

Results and discussion

TROSY based 4D triple resonance HNCACO/HNCOCA pulse sequences have been published before (Yang and Kay 1999; Konrat et al. 1999). We derived our 4D pulse sequences based on more recent 3D pulse sequences (Werner-Allen et al. 2006), due to the more favorable properties such as increased sensitivity, and the option for parallel MQ evolution. The latter becomes a significant advantage only when the experiments are measured with novel sampling methods, such as APSY, since they allow exploiting the maximally possible evolution time.

The data for the variant of the presented method with the 4D TROSY APSY-HNCACO and the 4D TROSY APSY-HNCOCA experiment was measured as 66 projections within 53 h. The GAPRO analysis was performed with parameters that allowed the inclusion of peaks close to the noise level, and led to 436 and 633 entries in the 4D HNCOCA and 4D HNCACO peak lists, respectively. Merging of the two 4D peak lists by $^{1}H^{N}_{i}$–$^{15}N_{i}$ correlation resulted in 314 inter-residue 6D $^{13}C^{\alpha}_{i-1}$–$^{13}C'_{i-1}$–$^{1}H^{N}_{i}$–$^{15}N_{i}$–$^{13}C^{\alpha}_{i}$–$^{13}C'_{i}$ spin systems using threshold ellipses with axes 0.05/0.2/0.2/0.2 ppm for $^{1}H^{N}/^{15}N/^{13}C'/^{13}C^{\alpha}$. The average difference of matched chemical shifts in the ^{15}N and the $^{1}H^{N}$ dimension was 0.03 and 0.002 ppm, respectively. The analysis by the MARS software (Jung and Zweckstetter 2004) resulted in a backbone assignment with a completeness of 85 %. The average difference of matched $^{13}C^{\alpha}$ and $^{13}C'$ chemical shifts was 0.03 ppm. Based on these values we could estimate the precision of chemical shifts in the APSY peak lists to be about 20 times higher than for conventional peak lists: these are usually limited to the spectral resolution of the spectra in which the peaks are picked. A more thorough discussion of the precision of chemical shifts in APSY peak lists can be found, e.g., in (Hiller and Wider 2011).

The same procedure was applied with the experiments that include $^{13}C^{\beta}$: Merging of the two 4D correlation list to a 6D $^{13}C^{\alpha}_{i-1}$–$^{13}C^{\beta}_{i-1}$–$^{1}H^{N}_{i}$–$^{15}N_{i}$–$^{13}C^{\alpha}_{i}$–$^{13}C^{\beta}_{i}$ peak list and automated assignment resulted again in a completeness of about 85 %. The result was robust with respect to a range of analysis parameters, as noted in the Supplementary Material. For the current application, a lower number of projections would have been sufficient for the same result, but would require more tedious parameter adjustments. The main time savings with this APSY method is the circumvention of labor-intensive and tedious manual assignment procedures which can take months. The measurement of a reasonable number of projection spectra (for details see the data sets in the Supplementary Materials) ensures the efficiency and reliability of the processing and analysis procedure.

The two sets of experiments have intrinsic features which differentiate their potential applications. The backbone experiments that do not include $^{13}C^{\beta}$ provide potentially higher sensitivity (see comparison in Fig. 3), in particular when applied with proteins obtained from media in D_2O with protonated glucose, where the $^{13}C^{\alpha}$ are almost fully deuterated whereas the $^{1}H^{\beta}$ are only partially (50–70 %) replaced by deuterons which reduces the sensitivity of experiments with $^{13}C^{\beta}$ evolution. Still, as a basis for a full resonance assignment the experiments that include $^{13}C^{\beta}$ will be used. However, the assignment of $^{13}C^{\beta}$ is often not necessary, e.g., when the backbone dynamics shall be investigated, hence the more sensitive pair of experiments can be used.

The combination of the peak lists of all four experiments to 8D spin systems and a subsequent MARS analysis resulted in a backbone assignment completeness of 90 %. 95 % of all residues had at least two chemical shifts assigned. The assignments of the different approaches were verified by comparing them and by checking the matching precisions. Using the verified assignment based on all experiments, we found that for the HNCACO/HNCOCA assignment all fragments with lengths of 4–48 residues proved to be mapped correctly to the protein sequence with the exception of two 4-residue fragments. The chemical shift information of these fragments was not characteristic enough to allow unambiguous placement onto the ORF904 sequence based on backbone chemical shifts only; the amino-acid specific chemical shift of $^{13}C^{\beta}$ could have helped in these cases. The completeness of the correct

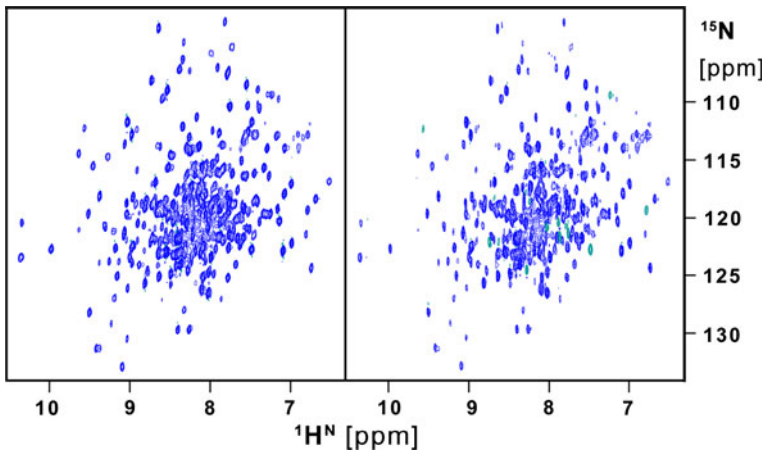

Fig. 3 Comparison of the 2D $^{1}H^{N}$–^{15}N projection spectra of a 4D TROSY APSY-HNCOCA experiment (*left*), and a 4D TROSY APSY-HN(CO)CACB experiment (*right*)

automated assignment was, however, still 85 % even without $^{13}C^{\beta}$ resonances. For sensitivity-limited cases, and especially for proteins with "backbone deuteration", the $^{13}C'$-experiments may often be favorable as a basis for backbone assignments.

The resolution of overlaps and the high precision that can be obtained with these experiments are particularly noteworthy when considering that ORF904 contains only 15 % of β-sheets, with the resulting poor dispersion of resonances. The high sensitivity of the experiments with ORF904 originates partially from the experimental temperature of 50 °C. However, at the magnetic field used the two APSY experiments could be measured significantly faster than conventional 3D versions of these two experiments with the same maximal evolution times, in spite of the additional dimension and the significantly higher precision of the resulting 4D information. In addition, often more 3D experiments are required for complete sequential resonance assignment. The short measurement time in our case leaves room for applications at lower temperatures or at other less favorable conditions.

For the deuterated 38 kDa ORF904 protein, the optimized 4D TROSY HNCACO/HNCOCA experiments or the 4D TROSY HNCACB/HN(CO)CACB experiments measured with APSY have proven to be powerful tools for the assignment of backbone resonances. We were able to significantly extend the molecular weight of proteins for which higher-dimensional experiments and automated assignment are feasible. The sensitivity and resolution of the presented 4D TROSY APSY experiments allowed automated assignment of 90 % of the protein backbone and $^{13}C^{\beta}$ resonances of ORF904, the archaeo-eukaryotic primase-polymerase of plasmid pRN1 (Beck et al. 2010). The procedure proved also highly efficient: a total of 5 days of acquisition and 3 days of analysis were sufficient to achieve the presented results for all four 4D experiments. If only one set of two complementary TROSY APSY experiments is measured, as will be sufficient for many applications, only half the time is required. In principle, the pulse sequences of these 4D experiments could also be used to acquire the full dimensionality spectra, e.g., using sparse sampling (Orekhov et al. 2003; Jaravine et al. 2008). However, we believe that their use with APSY was important for the success of the assignment. Artifacts arising from spectral reconstruction do not appear with APSY experiments; the processing algorithm GAPRO even eliminates common spectral artifacts and directly provides highly precise chemical shift values, which supply the basis for unambiguous matching and hence reliable automated backbone assignment.

Acknowledgments We thank Prof. Sebastian Hiller (Basel) for technical discussions. The Swiss National Science Foundation (SNSF) is gratefully acknowledged for financial support (projects 120048 and 140559).

References

Beck K, Vannini A, Cramer P, Lipps G (2010) The archeo-eukaryotic primase of plasmid pRN1 requires a helix bundle domain for faithful primer synthesis. Nucleic Acids Res 38(19):6707–6718. doi:10.1093/nar/gkq447

Brutscher B, Morelle N, Cordier F, Marion D (1995) Determination of an initial set of NOE-derived distance constraints for the structure determination of $^{15}N/^{13}C$-labeled proteins. J Magn Reson B 109(2):238–242

Coggins BE, Zhou P (2006) Polar Fourier transforms of radially sampled NMR data. J Magn Reson 182(1):84–95. doi:10.1016/j.jmr.2006.06.016

Emsley L, Bodenhausen G (1990) Gaussian pulse cascades—new analytical functions for rectangular selective inversion and in-phase excitation in NMR. Chem Phys Lett 165(6):469–476

Fiorito F, Hiller S, Wider G, Wüthrich K (2006) Automated resonance assignment of proteins: 6D APSY-NMR. J Biomol NMR 35(1):27–37. doi:10.1007/s10858-006-0030-x

Gardner KH, Kay LE (1998) The use of ^{2}H, ^{13}C, ^{15}N multidimensional NMR to study the structure and dynamics of proteins. Annu Rev Biophys Biomol Struct 27:357–406

Geen H, Freeman R (1991) Band-selective radiofrequency pulses. J Magn Reson 93(1):93–141

Gossert AD, Hiller S, Fernandez C (2011) Automated NMR resonance assignment of large proteins for protein-ligand interaction studies. J Am Chem Soc 133(2):210–213. doi:10.1021/ja108383x

Grzesiek S, Bax A (1993) The importance of not saturating H_2O in protein NMR—application to sensitivity enhancement and NOE measurements. J Am Chem Soc 115(26):12593–12594

Güntert P, Dötsch V, Wider G, Wüthrich K (1992) Processing of multidimensional NMR data with the new software PROSA. J Biomol NMR 2(6):619–629

Hiller S, Wider G (eds) (2011) Automated projection spectroscopy and its applications, vol 316 Topics in Current Chemistry. Berlin Heidelberg, Springer

Hiller S, Fiorito F, Wüthrich K, Wider G (2005a) Automated projection spectroscopy (APSY). Proc Natl Acad Sci USA 102(31):10876–10881. doi:10.1073/pnas.0504818102

Hiller S, Wider G, Etezady-Esfarjani T, Horst R, Wüthrich K (2005b) Managing the solvent water polarization to obtain improved NMR spectra of large molecular structures. J Biomol NMR 32(1):61–70. doi:10.1007/s10858-005-3070-8

Hiller S, Wasmer C, Wider G, Wüthrich K (2007) Sequence-specific resonance assignment of soluble nonglobular proteins by 7D APSY-NMR Spectroscopy. J Am Chem Soc 129(35):10823–10828. doi:10.1021/ja072564+

Hiller S, Joss R, Wider G (2008a) Automated NMR assignment of protein side chain resonances using automated projection spectroscopy (APSY). J Am Chem Soc 130(36):12073–12079. doi:10.1021/ja803161d

Hiller S, Wider G, Wüthrich K (2008b) APSY-NMR with proteins: practical aspects and backbone assignment. J Biomol NMR 42(3):179–195. doi:10.1007/s10858-008-9266-y

Jaravine VA, Zhuravleva AV, Permi P, Ibraghimov I, Orekhov VY (2008) Hyperdimensional NMR spectroscopy with nonlinear sampling. J Am Chem Soc 130(12):3927–3936. doi:10.1021/jao077282o

Jung YS, Zweckstetter M (2004) MARS—robust automatic backbone assignment of proteins. J Biomol NMR 30(1):11–23

Kay LE, Keifer P, Saarinen T (1992) Pure absorption gradient enhanced heteronuclear single quantum correlation spectroscopy with improved sensitivity. J Am Chem Soc 114(26):10663–10665

Kazimierczuk K, Zawadzka A, Kozminski W, Zhukov I (2006) Random sampling of evolution time space and Fourier transform processing. J Biomol NMR 36(3):157–168. doi:10.1007/s10858-006-9077-y

Kim S, Szyperski T (2003) GFT NMR, a new approach to rapidly obtain precise high-dimensional NMR spectral information. J Am Chem Soc 125(5):1385–1393. doi:10.1021/ja028197d

Konrat R, Yang DW, Kay LE (1999) A 4D TROSY-based pulse scheme for correlating (HN_i)-^1H,$^{15}N_i$,$^{13}C_i^{\alpha}$,$^{13}C_{i-1}'$ chemical shifts in high molecular weight [^{15}N,^{13}C,^2H]-labeled proteins. J Biomol NMR 15(4):309–313

Krähenbühl B, Wider G (2012) Automated projection spectroscopy (APSY) for the assignment of NMR resonances in biological macromolecules. Chimia 66(10):767–771

Krähenbühl B, Hiller S, Wider G (2011) 4D APSY-HBCB(CG)CDHD experiment for automated assignment of aromatic amino acid side chains in proteins. J Biomol NMR 51(3):313–318. doi:10.1007/s10858-011-9572-7

Kupce E, Freeman R (2003) Projection-reconstruction of three-dimensional NMR spectra. J Am Chem Soc 125(46):13958–13959. doi:10.1021/ja038297z

Marion D, Ikura M, Tschudin R, Bax A (1989) Rapid recording of 2D NMR spectra withoug phase cycling—application to the study of hydrogen-exchange in proteins. J Magn Reson 85(2):393–399

Narayanan RL, Dürr UHN, Bibow S, Biernat J, Mandelkow E, Zweckstetter M (2010) Automatic assignment of the intrinsically disordered protein Tau with 441 residues. J Am Chem Soc 132(34):11906–11907. doi:10.1021/ja105657f

Orekhov VY, Ibraghimov I, Billeter M (2003) Optimizing resolution in multidimensional NMR by three-way decomposition. J Biomol NMR 27(2):165–173. doi:10.1023/A:1024944720653

Pervushin K, Riek R, Wider G, Wüthrich K (1997) Attenuated T_2 relaxation by mutual cancellation of dipole–dipole coupling and chemical shift anisotropy indicates an avenue to NMR structures of very large biological macromolecules in solution. Proc Natl Acad Sci USA 94(23):12366–12371

Pervushin KV, Wider G, Wüthrich K (1998) Single transition-to-single transition polarization transfer (ST2-PT) in ^{15}N,^1H-TROSY. J Biomol NMR 12(2):345–348

Salzmann M, Wider G, Pervushin K, Wuthrich K (1999) Improved sensitivity and coherence selection for ^{15}N,^1H -TROSY elements in triple resonance experiments. J Biomol NMR 15(2):181–184

Shaka AJ, Keeler J, Frenkiel T, Freeman R (1983) An improved sequence for broad-band decoupling—WALTZ-16. J Magn Reson 52(2):335–338

Szyperski T, Wider G, Bushweller JH, Wüthrich K (1993) Reduced dimensionality in triple-resonance NMR experiments. J Am Chem Soc 115(20):9307–9308

Volk J, Herrmann T, Wüthrich K (2008) Automated sequence-specific protein NMR assignment using the memetic algorithm MATCH. J Biomol NMR 41(3):127–138. doi:10.1007/s10858-008-9243-5

Werner-Allen JW, Jiang L, Zhou P (2006) A 'just-in-time' HN(CA)CO experiment for the backbone assignment of large proteins with high sensitivity. J Magn Reson 181(1):177–180. doi:10.1016/j.jmr.2006.04.001

Wider G, Dreier L (2006) Measuring protein concentrations by NMR spectroscopy. J Am Chem Soc 128(8):2571–2576. doi:10.1021/ja055336t

Yang DW, Kay LE (1999) TROSY triple-resonance four-dimensional NMR spectroscopy of a 46 ns tumbling protein. J Am Chem Soc 121(11):2571–2575